Geoscience Frontiers 15 (2024) 101894

Contents lists available at ScienceDirect

Geoscience Frontiers

journal homepage: www.elsevier.com/locate/gsf

Research Paper

Gravitational and elastic energies stored in crustal volumes activate normal versus strike-slip and thrust seismogenic faults

Carlo Doglioni [a,b,*]

[a] Dipartimento Scienze della Terra, Sapienza University, Rome, Italy
[b] Istituto Nazionale di Geofisica e Vulcanologia, Rome, Italy

ARTICLE INFO

Article history:
Received 22 April 2024
Revised 6 June 2024
Accepted 12 July 2024
Available online 14 July 2024
Handling Editor: R. Damian Nance

Keywords:
Pro-gravity tectonics
Iso-gravity tectonics
Counter-gravity tectonics
Graviquake
Elastoquake

ABSTRACT

Shallow crustal faults are passive features mobilized by the dissipation of the potential energy and the shear stress accumulated in the brittle volume surrounding them. However, the stored energy in the volume differs from the tectonic setting, i.e., it is mainly gravitational in extensional tectonic settings, whereas it is elastic in strike-slip and contractional tectonic environments. In extensional settings, below about 1 km, the horizontal tensile stress is overwhelmed by the confining pressure of the lithostatic load, and it becomes positive, i.e. compressive. Therefore, there is no horizontal tension in extensional tectonic settings and the pro-gravity motion of the crustal volume is provided by the lithostatic load, which is the vertical maximum principal stress. The elastic energy is rather accumulated by the maximum horizontal principal stresses, i.e., iso-gravity in transcurrent settings and counter-gravity in contractional tectonic settings. The different relation with the gravitational force in the different tectonic settings generates several relevant differences in the three main tectonic environments. The extensional tectonic settings, both in continental and oceanic rift zones generate normal fault-related earthquakes, i.e., pro-gravity movements, or graviquakes. They differ from the other tectonic setting because are marked by (i) lower energy and lower differential stress to activate faults with respect to strike-slip and contractional tectonics; (ii) lower maximum earthquake magnitude; (iii) a larger number of low magnitude earthquakes in extensional settings because the crust moves downward as soon as it can move, whereas contractional settings require larger accumulation of energy to move counter-gravity; (iv) consequently, the *b*-value of the Gutenberg-Richter is higher than 1 and the aftershocks are more numerous and last longer in extensional settings; (v) the downward motion of the hangingwall determines more diffuse cataclastic deformation with respect to the other tectonic settings because the lithostatic load works everywhere, whereas in the other tectonic settings is concentrated where the elastic energy accumulates; (vi) in extensional settings the volume dimension is determined by thickness of the brittle layer, and its length is in average three times the seismogenic thickness; in strike-slip and contractional settings dominates the elastic energy (elastoquakes), and the mobilized volume may be ten to thirty times longer in a single seismic sequence, being its size proportional both to the brittle thickness and the relative speed of plates. These differences characterize the seismic cycle of graviquakes with respect to the elastoquakes. The bigger the volume, the wider the seismogenic fault in all tectonic settings. The interplay between the horizontal tectonic forces and the lithostatic load, which is ubiquitous, varies in the three main tectonic settings, generating different seismotectonic styles and an increase of magnitude as the effect of the vertical gravitational force becomes a minority relative to the elastic storage and coseismic rebound.

1. Introduction

Seismology does not differentiate the energy determining fault activation and the consequent release of elastic waves (Bath, 2013). Earthquake studies mostly focus on the main faults that generate them, i.e., their focal mechanism, the fault shape and dimension, the static and dynamic friction, and all the possible measurable geophysical parameters (e.g., Stein and Wysession, 2009; Scholz, 2019). However, crustal faults and related seismicity show several differences as a function of their tectonic settings. This research tries to discuss some of them, concentrating on the

* Address at: Dipartimento Scienze della Terra, Sapienza University, Rome, Italy.
E-mail address: carlo.doglioni@uniroma1.it

https://doi.org/10.1016/j.gsf.2024.101894

brittle shallow crust. Faults are passive discontinuities (Bignami et al., 2020) delivering a tiny part of the energy stored in the surrounding crustal volume (Sornette, 1999; Kanamori and Rivera, 2006; Doglioni et al., 2011, 2015a; Johnson et al., 2021). This study is a sequel of a number of articles proving theoretically and with data how different forces are responsible for fault activation, particularly demonstrating how in extensional tectonic settings the main energy stored in the crustal volume is mostly gravitational and not elastic as in the other geodynamic settings (Doglioni et al., 2011, 2015a, 2015b; Thompson and Parsons, 2017; Bignami et al., 2019, 2020; Petricca et al., 2021, 2022). Moreover, the theory predicts tensile elastic stress acting on the fault interface and rock volumes beside it. However, in extensional tectonic settings, the σ_1 coincides with the lithostatic load, i.e., the gravitational energy (Fig. 1) and modeling and borehole well logs show that the σ_3 is contractional below few hundred meters (Twiss and Moores, 1992; Zoback et al., 1993), preventing any horizontal tensile stress in the crust, regardless the lithosphere is spreading apart (Fig. 2). Moreover, stress concentration varies with lithologies and depth (Shebalin and Narteau, 2017). Therefore, differentiating normal faults where the vertical principal stress is the lithostatic load (i.e., the gravitational force) with respect to the other tectonic settings where the elastic energy activates the crustal volumes may help further to understand the mechanics and evolution of the seismic cycle. The three main tectonic settings, i.e., extensional, strike-slip and compressional, require respectively increasing differential stress to activate faults (Fig. 1). The classic formulation of Sibson (1974) predicts

$$\sigma_1 - \sigma_3 = \beta\rho g z(1-\lambda) \quad (1)$$

where σ_1 is the maximum principal stress, σ_3 is the minimum principal stress, β is a parameter of 0.75, 1.2, and 3 respectively in normal, transcurrent and reverse faulting, ρ is the crustal density, g is the gravitational acceleration, z is the depth, and λ is the fluid pressure. Elastic rebound is assumed to be the common mechanism in all tectonic settings (Reid, 1911). However, why each tectonic setting requires specific differential stress? The seismicity associated with the three tectonic settings show separated Gutenberg-Richter (GR) b-value, i.e., 1.1, 1 and 0.9, for extensional, strike-slip and contractional tectonics respectively (Schorlemmer et al., 2005), and the correlated Omori p-value (Narteau et al., 2009; Zaccagnino et al., 2022). This is consistent with a lower potential maximum magnitude for normal faults (around M_w 7.5) with respect to strike-slip (M_w 8.7) and thrusts (M_w 9.5), as suggested by Doglioni et al. (2015a). Therefore, the straight line of the logarithmic earthquake frequency versus magnitude of the Gutenberg-Richter law, i.e., defining the b-value, is steeper for normal faults, and shallower for thrusts. Hence, the b-value negatively correlates with the differential stress, which is lower in extensional tectonic regimes, and higher in contractional tectonic settings, being this relation still not entirely understood (Petruccelli et al., 2019). The usual assumption about coseismic rupture is that the differential

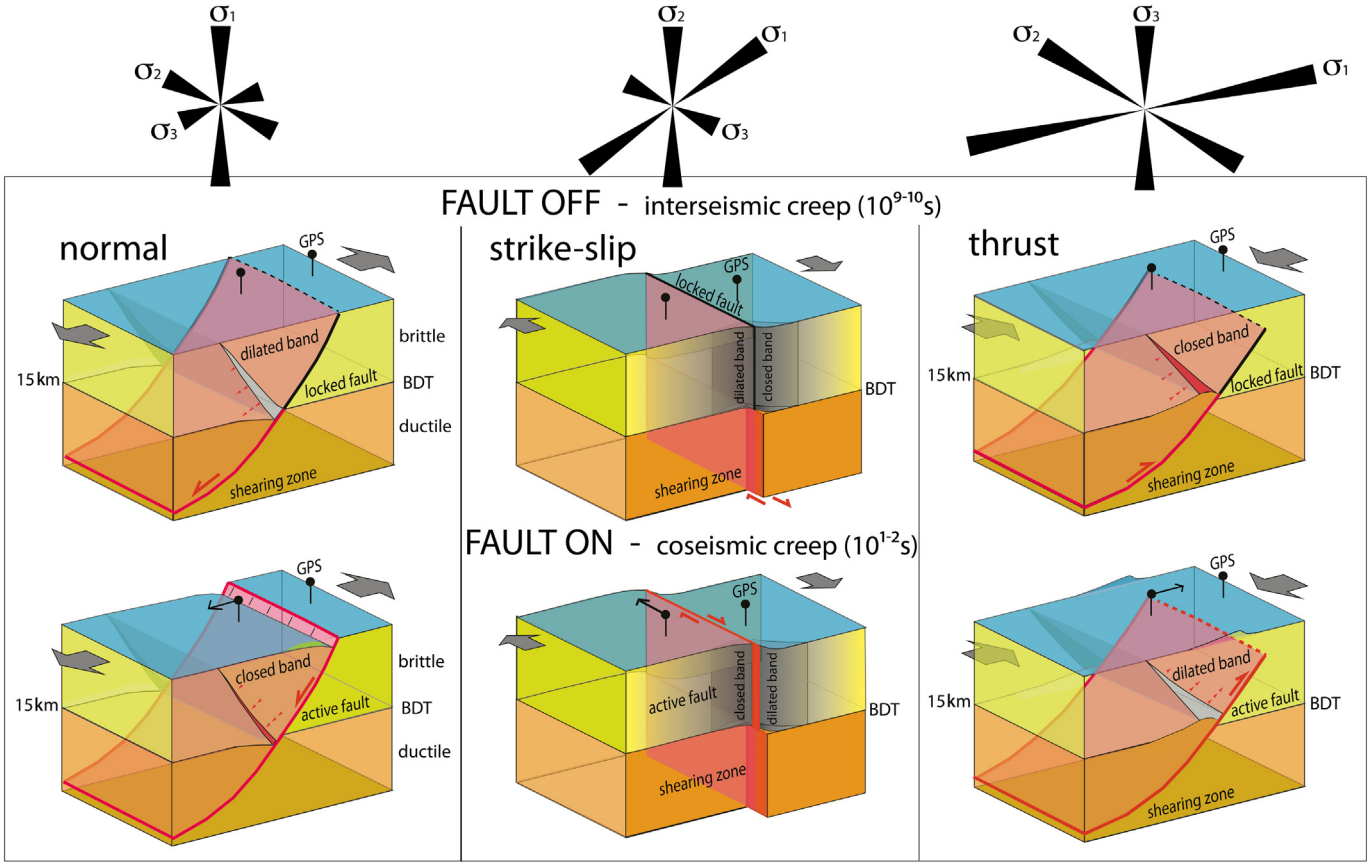

Fig. 1. Geological model of fault on–off in the three main tectonic settings. During the interseismic period (fault off), the brittle-ductile transition (BDT) separates the elastic-frictional (brittle) upper crust, where the faults are almost locked, from their related deeper shear zones, which are instead constantly creeping in the quasi-plastic (ductile) lower crust. GPS sites at the surface show no motion between the two walls of the faults (upper figures). The upper crust above the BDT suffers dilation in the normal fault case, shortening in the thrust fault case, and two opposite bands of dilation and shortening in the strike-slip fault. During the coseismic stage (fault on), the faults of the brittle upper crust are activated, and the conjugate bands above the BDT experience opposite kinematics, i.e., the dilated volume is compressed, and the compressed volume is dilated. The bands that formed during the interseismic stage above the BDT at a high angle relative to the main fault, may evolve into conjugate faults (modified after Doglioni et al., 2015a).

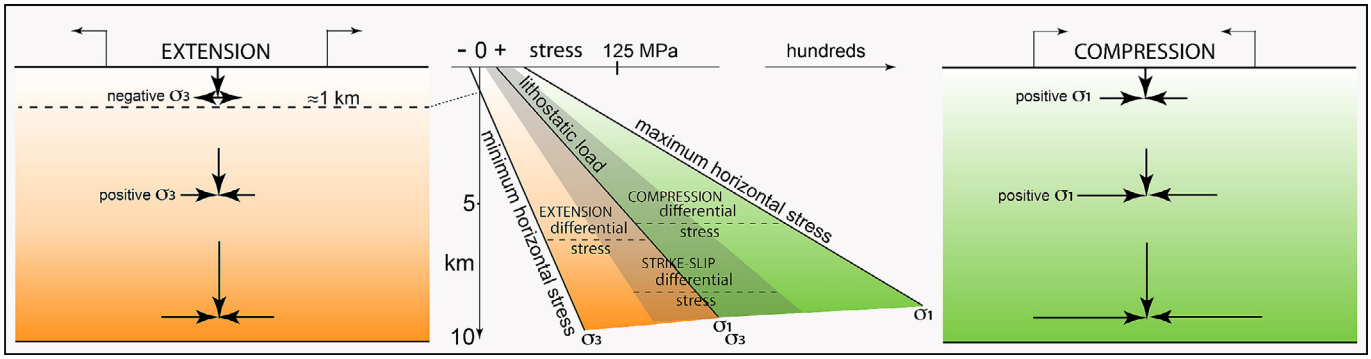

Fig. 2. In extensional tectonic settings, the minimum stress tensor (σ_3) generates horizontal traction only above 1 km of depth, where it is negative. Below that depth it becomes positive, i.e., the crust is in compressive state even in rifting areas due to the increase of the confining pressure generated by the vertical lithostatic load. Here an average density of 2.5 g/cm^3 and an increase of the lithostatic load of 25 MPa/km is assumed. The area between the lithostatic load and the minimum horizontal stress represents the deviatoric stress and contains the stress data measured in wells. To the right, the compressional tectonic setting in which contraction of the crust occurs also at shallow depth. Strike-slip setting is in the middle shadow area.

stress equals the Coulomb-Griffith criterium, being all tectonic settings controlled by elastic energy. Sibson (1977) estimated the value of elastic energy (E), being roughly proportional to the differential stress, where σ_1 is the maximum principal stress and σ_3 is the minimum principal stress:

$$E \propto (\sigma_1 - \sigma_3) \quad (2)$$

A difference in the b-value between compression and extensional tectonics has been also recognized in Italy (Taroni and Carafa, 2023). Moreover, the ratio between the crustal seismogenic thickness and the horizontal length of the moving volume, and the related faults varies from 2 to 4 for normal faults, 9 to 15 for strike-slip, and up to even more than 25 for thrusts (see Doglioni et al., 2015a for discussion and data). Despite the lower maximum magnitude of the related earthquakes, normal faults show much thicker fault damage zones with respect to thrusts (Zaccagnino and Doglioni, 2022a). Why there are all these differences? Megathrusts and $M > 9$ occur only along subduction zones, where the coalescence of the upper-lower plate decollement determines thrust activation that may be even more than one thousand km long, e.g., the 1400 km long Sumatra-Andaman 2004 M_w 9.2 event, (Lay et al., 2005; Pollitz et al., 2008), or the Tohoku 2011 M_w 9.1 earthquake with non-uniform slip that extended ~220 km across the width and ~400 km along strike of the central-northern Japan subduction zone, that is shorter but wider, with a seismogenic thickness of about 30 km, tapering toward the east (Lay, 2018). Normal faults are much shorter surfaces, rarely exceeding 50–60 km of coseismic rupture (Beanland et al., 1990), being highly undulated or fragmented (Searle et al., 2010), and further interrupted by transform faults every few hundred km or less in the oceanic rifts or associated to transfer zones along the major continental rifts worldwide, e.g., the Mid Atlantic Ridge (Allerton et al., 1995), or the East Africa Rift (Morley, 1988). Strike-slip faults have lengths in between, reaching a few hundred km of coseismic rupture like the 2023 M_w 7.8 Turkish-Syrian earthquake along the Eastern Anatolia Fault system (Chen et al., 2023). The different tectonic settings characterize plate boundaries and shape the Earth's surface differently moving the crust pro-, iso- and counter-gravity (Fig. 3). Crustal earthquakes are the sudden release of seismic radiation associated with the friction on fault planes of the stress accumulated in the seismogenic volume due to the slow action of tectonic forces (Kanamori, 1994; Kanamori and Brodsky, 2004; Scholz, 2019). While damages tend to occur at the interface of geological units with contrasting rheological properties so that mechanically weaker points are spatial fractals (Kagan, 1991; Ben-Zion and Sammis, 2003; Telesca and Lapenna, 2006) with surface-like appearance at large scales, energy is accrued in the adjoining volumes (Muir Wood, 1994; Pearson et al., 1995; Doglioni et al., 2015b; Okubo et al., 2019; McBeck et al., 2022). Both the events develop with strongly nonlinear behaviors in time and with extreme heterogeneity in space provoking rock failures once they are not compatible with each other, i.e., if the weakest segment of the system cannot hold local stress anymore (Biswas et al., 2015).

Hence, earthquakes contribute to reaching a new state of stability via stress dissipation, also reducing the energy accumulated due to the motion of contiguous crustal volumes with respect to each other. The dynamics of seismic events show large variability depending on the physical properties of the geological environment, ranging from episodic tremors and slip along the shallow section of the subduction zones to complex seismic sequences in intraplate fault systems. Furthermore, fluid circulation in the surroundings of active fault systems is tied to the seismic cycle through a chain of processes, leading to a complex interaction between fracturing, chemical alternations and changes in friction and permeability. Opposite patterns in fluid flows are predicted in compressive and extensional tectonic settings during the different phases of seismic activity (Muir-Wood and King, 1993; Doglioni et al., 2014), with large amounts of liquids ejected from rifting areas in the post-seismic period (Chiarabba et al., 2022). The redistribution of fluids in space is driven by a dilatant behavior of rocks while accommodating progressive stress variations during the interseismic and pre-seismic phases and by dramatic, sudden changes in pressure after large seismic events causing violent water discharge and often significant offsets in the reference level of springs. Unlike brittle crustal seismicity, deep subduction events or intraslab seismicity showcase quite different stress orientations and energy release as a function of the subduction geographic polarity (Doglioni and Panza, 2015), and may have important magnitudes (Jiménez, 2018), but pertain to other deformation settings which are out of the scope of this analysis.

2. Energy models

The energy and earthquake magnitude scales with the involved volume and the resulting fault length (Doglioni et al., 2011, 2015a; Petricca et al., 2022). The work done in lifting upward a crustal volume and the work done by gravity as it falls downward are equal in magnitude but opposite in sign. However, the work done to move the crustal volume upward requires the input of energy, while the work done by gravity during the hanging wall descent releases the stored potential energy as kinetic energy, which does not require

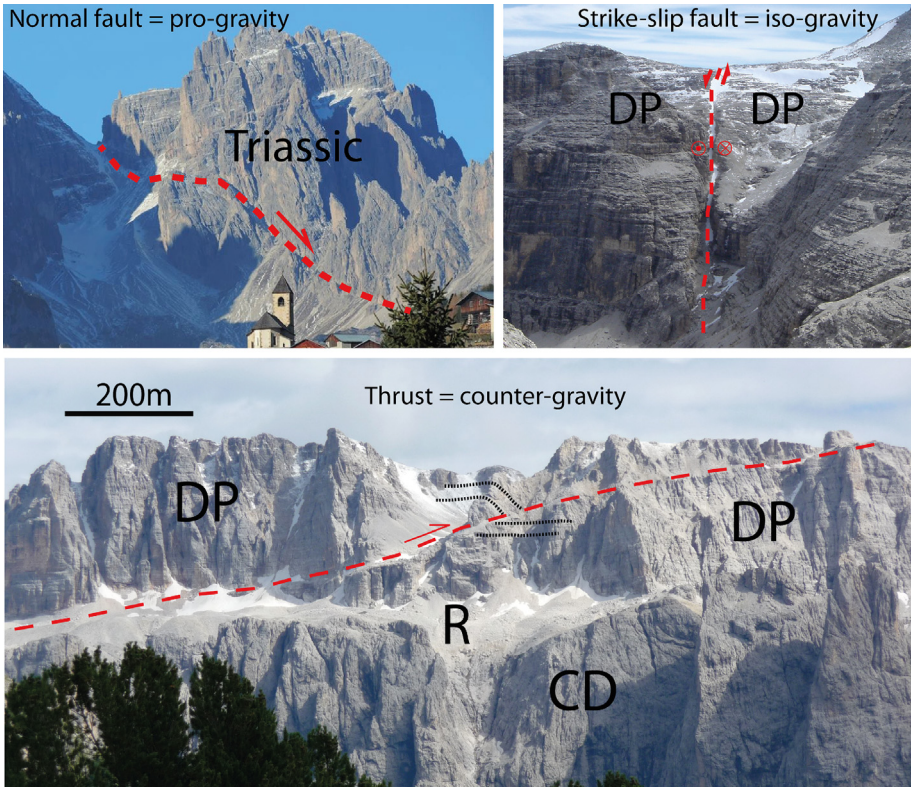

Fig. 3. Examples of the three classic tectonic settings from the Dolomites, northern Italy. The normal fault (north of Sappada), strike-slip fault and thrust (Sella Group) mostly affect Triassic carbonates, such as the Dolomia Principale (DP), Raibl Fm (R) and Cassian Dolomite (CD). The three settings move in favor of gravity, in iso-gravity, or against gravity, respectively.

to be supplied by the tectonic system. Both movements need the shear stress on fault to overcome the resisting friction at the onset of the coseismic slip.

Seismological modeling is grounded on the elastic rebound model (Reid, 1911). Under the assumption of mechanically homogeneous materials, fault dynamics is thought to be controlled by an almost periodic cycle of accumulation and discharge of elastic energy at the fault interface and surrounding volumes. By this viewpoint, compressive and extensional tectonic settings should share the same seismic dynamics, being also completely indistinguishable from that of strike-slip regions. However, in extensional tectonic settings, the horizontal tensile stress disappears even shallower than 1 km depth (Bignami et al., 2020), i.e., the crustal layers are in contraction below even less than 1 km depth. Therefore, along rift areas, the gravitational energy E determines the hanging wall coseismic collapse, and the seismic radiation increases with the volume dimension and the fault dip (Doglioni et al., 2015a, 2015b; Bignami et al., 2019, 2020):

$$E \propto (\sigma_1 - \sigma_3) \propto mgh(\mu_s, \Theta) \tag{3}$$

being m the mass of the hanging wall, g the gravitational acceleration, h the coseismic displacement, μ_s the static friction and Θ the fault dip. The fault dip tends to be 30° relative to the maximum principal stress (Sibson, 1974) and it may represent the angle with the largest shear stress gradient (Zaccagnino and Doglioni, 2023). However, mgh is the total amount of gravitational energy of the hanging wall under the assumption that the hanging wall is "floating in the air", while it should be considered that it is just lying in a weakened crustal volume close to the fault interface with widespread fractures filled with fluids; hence, the factual energy could be somehow slightly smaller than mgh. The gravitational collapse of the hanging wall is justified by the about one order of magnitude larger coseismic subsidence with respect to the uplifted footwall and hanging wall areas (Valerio et al., 2018; Bignami et al., 2019). This model has been tectonically supported by the occurrence of antithetic bands permeated by diffused interseismic dilatant fracturing that allows coseismic contraction (Doglioni et al., 2011, 2015a).

Therefore, the extensional tectonic settings provide a different energetic source with respect to strike-slip and compressional tectonic settings where the elastic energy rather dominates (Fig. 4).

The following two formulae (modified after Doglioni et al., 2015b) quantify the elastic energy required for strike-slip (4) and contractional settings (5), where E is the energy, K is the bulk modulus, V is the hanging wall volume (for thrusts and normal faults) and the adjacent volumes for strike-slip faults, μ_s the static fault friction, Θ the fault dip, m the mass and ρ the density:

$$E = \frac{1}{2} K \left(\frac{\Delta V(\mu_s, \Theta)}{V} \right)^2 V \tag{4}$$

$$E = \frac{1}{2} K \left(\frac{\Delta V(\mu_s, \Theta)}{V} \right)^2 \frac{m}{\rho} \tag{5}$$

Let's take a brittle crustal volume 30 km long, 15 km thick and 10 km wide in the hanging wall of a thrust dipping 30°. The rocks have a density ρ of 2600 kg/m^3 and the static friction μ is 0.7. Let's assume that the coseismic average slip determines an uplift of 2 m. Therefore, the volume is 2250 km^3 and the mass is 5.85×10^{15} kg. The work required for moving that mass is 1.27×10^{17} Joule.

Let's now assume the same volume moving 2 m downward along a normal fault dipping 60° and having the same friction. The work expenditure will be 5.96×10^{16} Joule. The values are not necessarily the same due to the different dip and motion relative to gravity. In compressional tectonics, it is required to accumulate elastic energy to move the volume against gravity plus the

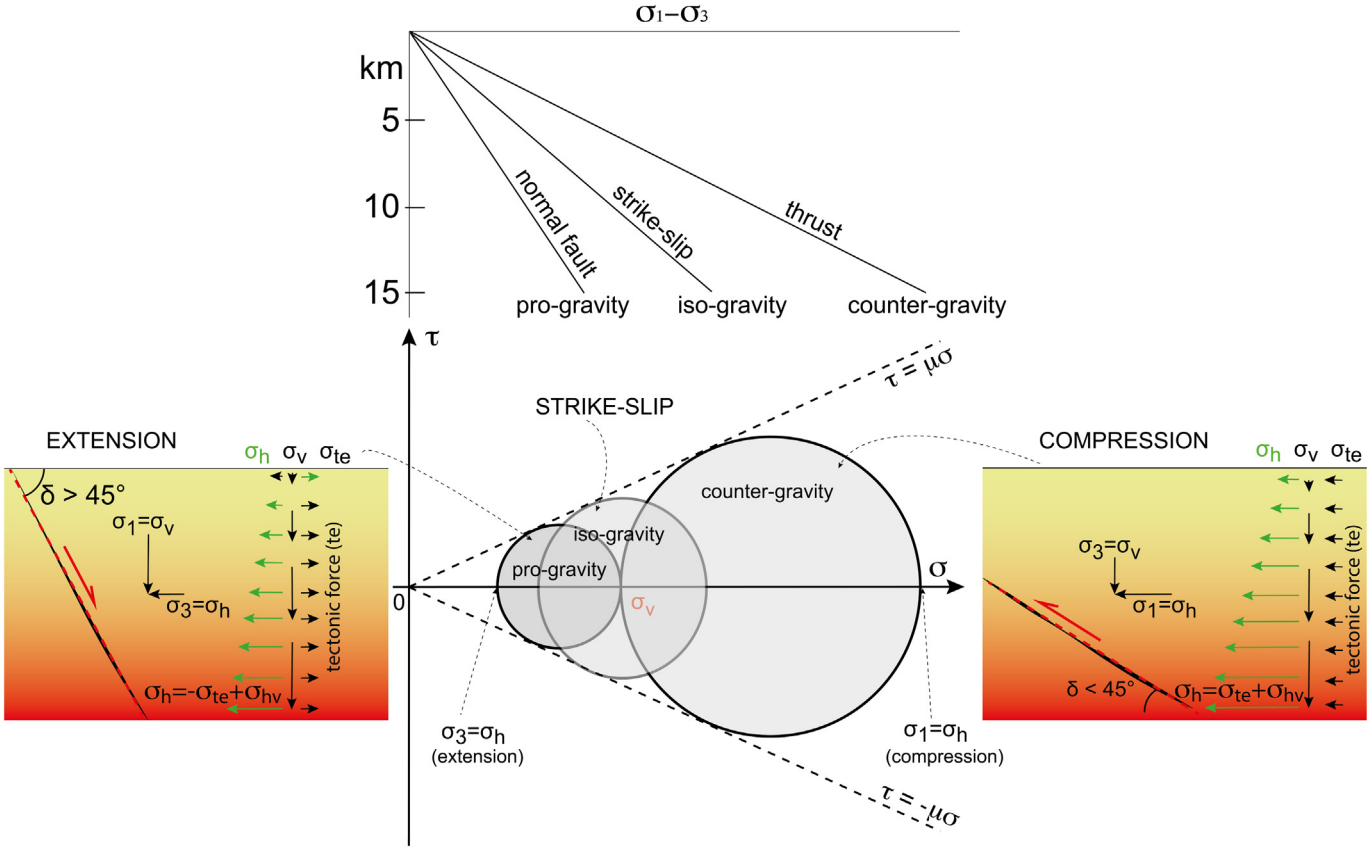

Fig. 4. Mohr circles in the three main tectonic settings. They increase in diameter, i.e., the differential stress, moving from the extensional, wrenching and compressional tectonic settings. The horizontal stress (σ_h) is the sum of the tectonic stress (σ_{te}) plus the confining pressure deriving from the lithostatic load (σ_v). Notice that even in extensional tectonic settings the minimum stress (σ_3) is positive, i.e., contractional. Notice that at any given depth, the lithostatic load represents the maximum stress field (σ_1) in extensional tectonic environments and the minimum stress field (σ_3) in contractional tectonic settings. The slope of the failure criterium τ is determined by the friction (μ) and the stress (σ). Upper panel, the differential stress required to activate normal, strike-slip and thrust faults increases in the three tectonic settings and may be related to the different control of the lithostatic load, i.e., favoring or pro-gravity (normal fault), being neutral or iso-gravity (strike-slip fault) and contrasting or counter-gravity (thrust) the hanging wall movement.

energy to overcome the friction. In extensional tectonics, the gravitational energy is instead in favor of motion plus again the energy required to overcome static friction. It was computed that the magnitude equivalent of the energy dissipated by the gravitational collapse is far greater than the real measured magnitude momentum (Kanamori and Rivera, 2006; Doglioni et al., 2011, 2015b), indicating that (1) the lithostatic load provides an energy budget that is far more than enough to activate the hangingwall downward movement along normal faults and (2) the remaining part of energy not radiated by seismic waves is dissipated in shear heating, fracturing and folding of the rocky volume.

Furthermore, the differential stress required to activate a normal fault is much smaller than the ones of strike-slip and thrust faults as graphically evident since the σ_1 is the σ_3 of compressional settings (Fig. 4). Therefore, under the assumption of continuous, uniform distribution of materials in the faulting region and its surroundings, since the differential stress (variable with depth) is lower for extensional tectonic settings, also the energy is lower than the other tectonic settings to move the crustal volume and activate the fault(s). Since gravitational energy is everywhere, the deformation associated to normal faulting is more diffuse (Fig. 5).

3. Differences between extensional earthquakes and other tectonic settings

The difference between shallow crustal tectonic settings in terms of energy is compatible with several independent observations, such as the damage zone along the fault zones, the number of earthquakes during the interseismic period and the aftershock sequences (Narteau et al., 2002; Holschneider et al., 2012; Hatano et al., 2015; Zaccagnino et al., 2022), the relationship with topography, and the double-couple signature, that is larger in contractional settings. The more diffuse cataclastic deformation in extensional tectonic settings relative to the other tectonic settings can be attributed to the ubiquitous gravitational force.

It was shown that the fault gouge, the width of the fault the damage zone and the number of faults are larger along extensional areas with respect to contractional ones (Zaccagnino and Doglioni, 2022a, 2022b). The spacing of normal faults worldwide is generally narrower for normal faults (4–6 km) with respect to thrusts that may range between 5–25 km (Morellato et al., 2003). The fault spacing and its self-similarity depend on the seismogenic thickness in extensional settings, being larger with thicker brittle layer thickness. In contractional tectonics, e.g., in accretionary prisms, the thrust spacing rather increases with the deepening of the decollement layer (Boyer and Elliott, 1982; Boyer, 1995). However, the larger ruptures having the biggest volumes and higher magnitude earthquakes occur along subduction zones at the plate interface. The faster the convergence rate, the higher the expected magnitude.

It is simply counted here the number of earthquakes that can be detected in areas of a 30 km radius having a similar 2nd invariant strain rate of about 30–40 nanostrain (Riguzzi et al., 2012, e.g., 1.5–2 mm/yr either in contraction or in extension) and similar magnitude of completeness. See for example two Italian areas, one in

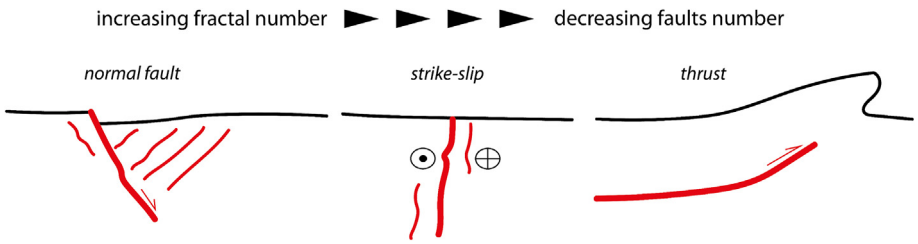

Fig. 5. Extensional tectonic settings show more faults and wider damage zones with respect to contractional environments. The spacing of normal faults is generally shorter and the fractal dimension tends to be lower due to more frequent secondary faults and fractures.

contraction and the second in extensional tectonic regime. Since January 1st 1985, the first area experienced 336 earthquakes, whereas the second 1962 events (Fig. 6). Adopting $M \geq 2$ as a threshold, the contractional area recorded 124 events, whereas the extensional one was 764, six times more. This simple comparison agrees also with aftershocks evolution of contractional and extensional regimes, being counter-gravity or pro-gravity; for comparable magnitude, normal fault-related seismic sequences last much longer and have a higher number of aftershocks because they move in favor of gravity that never stops, whereas the hanging-wall of a thrust ends moving as soon as the elastic energy required to move against gravity is consumed (Valerio et al., 2017). Moreover, this asymmetry fits with the different *b*- and *p*-values of contractional versus extensional tectonic settings as proposed by Zaccagnino et al. (2022) and redrawn in Fig. 7.

Furthermore, seismicity appears more concentrated along thrust planes with respect to extensional settings. This is a natural outcome of the different types of energy because gravitational energy is present everywhere, whereas, to generate a significant thrust earthquake, the elastic energy must be concentrated in each elongated and narrow hanging wall. See for example the extensional seismicity distributed all over the Basin and Range with respect to the one along the crustal section of subduction zones, where earthquakes are concentrated along the external belt with

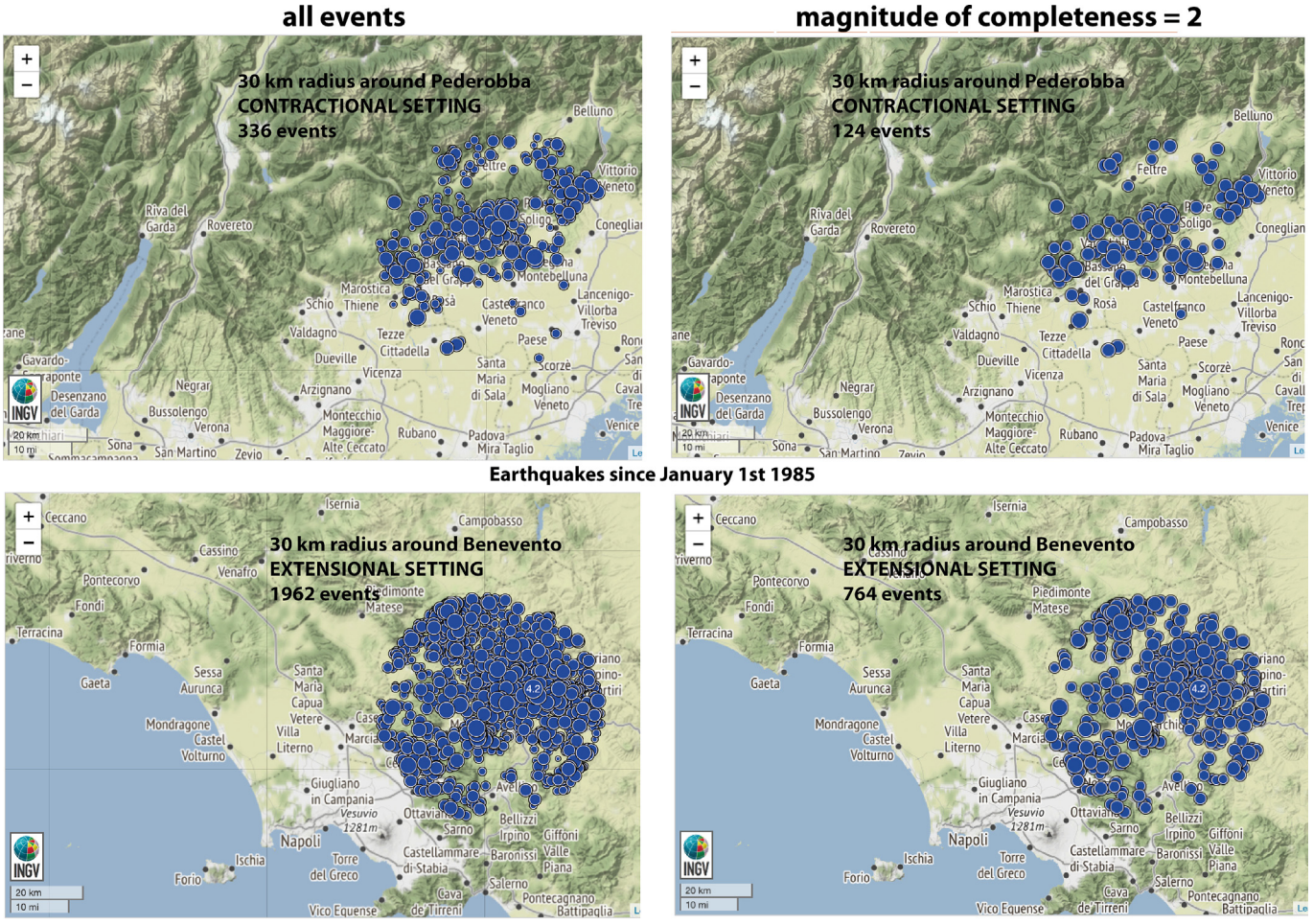

Fig. 6. Steady-state seismicity, without significant mainshocks from January 1st 1985 to May 11, 2023, from two examples of the Southern Alps (northern Italy) in compression, and of the southern Apennines in an extensional setting. Both areas show about 2 mm/yr of contraction and dilatation respectively, with 2nd invariant strain rate of about 20–30 nanostrain. Both areas have a similar magnitude of completeness of about 1.5–2. Notice how the extensional setting recorded about six times more earthquakes than the compressional one. To the left all the events in the catalogue and to the right the events $M \geq 2$. Data from http://terremoti.ingv.it/.

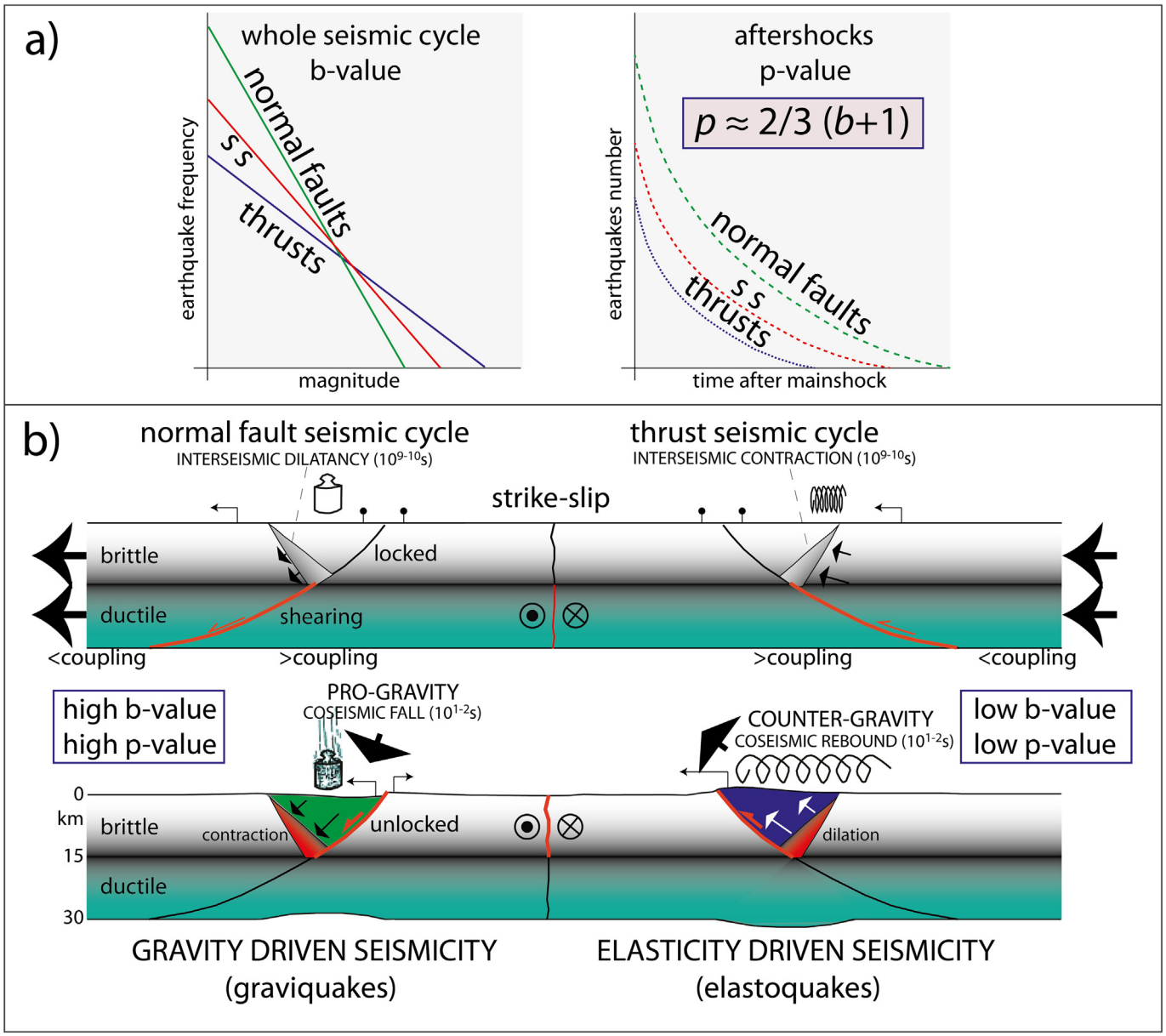

Fig. 7. (a) Left panel, the *b*-value of the Gutenberg–Richter law differs as a function of the tectonic setting, being higher in extensional tectonic settings. Therefore, normal faults have a steeper alignment, which means more low-magnitude events and lower maximum-magnitude earthquakes with respect to strike-slip (SS) and thrust faults; the right panel, being the *p*-value of the Omori law correlated to the *b*-value, shows different aftershocks evolution in time depending on the tectonic settings. On the basis of theoretical considerations and statistical analysis of one hundred seismic sequences, the most reliable relationship between them reads $p \approx 2/3\ (b + 1)$. Larger *p*-values mean that seismic dynamics move more rapidly towards stability, which also implies a relatively higher probability of secondary ruptures and more numerous aftershocks than the average reference. (b) A geological interpretation of different scaling behaviors can be given in light of different contributions to energy balance in the long-term rock volume mobilization. Contractional settings require more energy to move against gravity (adapted from Zaccagnino et al., 2022).

the lowest topography, i.e., the smaller lithostatic load σ_3. Also the double couple is larger for contractional tectonic settings, and both the Gutenberg-Richter and Omori parameters differ as a function of the tectonic setting (Zaccagnino et al., 2022; Zaccagnino and Doglioni, 2022a).

Therefore, the pro-gravity movements, or graviquakes, need less energy to mobilize volumes and activate the bounding faults with respect to the other tectonic settings if a dilatational volume is present at depth, to accommodate the extra volume lost at the surface (Bignami et al., 2019, 2020). The gravitational energy provided by the lithostatic load is everywhere, whereas the strike-slip and contractional settings need accumulation in time along plate boundaries or intraplate volumes where velocity gradients occur. The lithostatic load exerts control in the activation of thrust faults because they are active where the gravitational load is at its minimum, i.e., in the foothills or at the forefront of accretionary prisms and thrust belt fronts. This can be explained by the enlargement of the Mohr circle to the left approaching the failure criterium due to the lowest values of σ_3, i.e., the lithostatic load (Carminati et al., 2004).

Normal faults generate earthquakes of magnitude lower than the other tectonic settings. As shown before, this cannot be ascribed to the lower energy required to break rocks under traction, because the crust is in the contractional state even in extensional tectonic settings. We may infer the lower magnitude due to the easier volume mobilization and energy dissipation of smaller volumes in extensional settings because the gravitational load is always active everywhere. This can explain also the aforemen-

tioned larger number of normal fault-related earthquakes with respect to the contractional tectonic settings. This observation, linked with the lower maximum magnitude of extensional earthquakes determines the higher (>1) *b*-value of the Gutenberg-Richter for normal faults.

4. Discussion

Various combinations of stress sources produce the wide range of faulting styles routinely observed in the brittle lithosphere. Geological and seismological differences among tectonic settings are usually related to frictional properties of faults and profiles of differential stress. In the present paper, we analyze this issue from a different viewpoint, considering how tectonics is heavily controlled by gravitational forces, favoring deformation in extensional settings, and contrasting shortening in contractional tectonic settings. It was formerly discussed the total energy budget activating crustal volumes and the related faults. The energy generates the differential stress, which varies with depth and is the result of the interplay between horizontal tectonic forces and the lithostatic load increasing with depth. The differential stress required to activate a fault system is lower in extensional tectonic settings with respect to strike-slip and contractional tectonics. Coherently, thrust-related earthquakes may reach two degrees of moment magnitude higher than the normal faults. This is usually interpreted because breaking rocks under contraction requires more energy than under traction. However, in the crust beneath 1 km, rocks are under compression also in extensional tectonic settings due to the confining pressure exerted by the lithostatic load. The differential stress is larger in contractional settings because the hanging wall volume moves against gravity, requiring much larger energy with respect to extensional settings where the volume moves in favor of gravity. Seismological parameters follow this energetic constraint, e.g., the interseismic larger number of earthquakes of low magnitude in extensional tectonic settings and longer aftershocks following normal fault mainshock with respect to contractional areas with similar 2nd invariant strain rate. Therefore, the *b*-value of the Gutenberg-Richter and the *p*-value of the Omori laws are higher in extensional settings.

In all tectonic settings, the energy is mostly stored in the volume adjacent to faults, i.e., the hangingwall for normal faults and thrusts, or both walls adjacent to sub-vertical strike-slip faults. In this view, faults are passive weakness zones where seismic radiation occurs due to the friction on the surfaces. Rupture starts from the weakest area of the main fault plane, improperly called asperity.

The elastic energy radiated by earthquakes is notoriously a smaller amount of the entire energy budget accumulated and released during the coseismic motion (e.g., Doglioni et al., 2015a). The stress drop is the difference between the stress across a fault before and after an earthquake rupture, and therefore may represent only a tiny part of the energy budget dissipated during the rupture. However, Cocco and Rovelli (1989) have shown that the stress drop in compressional settings is far higher than in extensional tectonic environments. This is consistent with the larger energy budget required to shift the crust counter-gravity.

It was observed that in extensional tectonic settings, the rupture tends to start in the lower part of the fault plane and propagate upward and laterally, whereas in compressional tectonic settings, it is the opposite, i.e., it preferentially initiates at a shallow level and propagates downward and laterally due to the opposite control of the lithostatic load, which favors normal faulting, whereas it contrasts thrusting (Carminati et al., 2004). This is consistent with the largest energy accumulation for the lithostatic load (maximum principal stress, σ_1) in the lower part of the hanging wall volume in extensional settings and the differential stress enlarges to the right in the Mohr circle, whereas in contractional tectonic environments, the shallow layers have the minimum lithostatic load, determining a shift to the left of the differential stress (minimum principal stress, σ_3) and favoring the contact with the failure criterium (Fig. 7). Therefore, topography matters in triggering fault activation. In fact, normal faults show bottom-up rupture propagation (e.g., Li et al., 2023), whereas thrusts exhibit more frequent top-down coseismic rupture migration (e.g., Koketsu

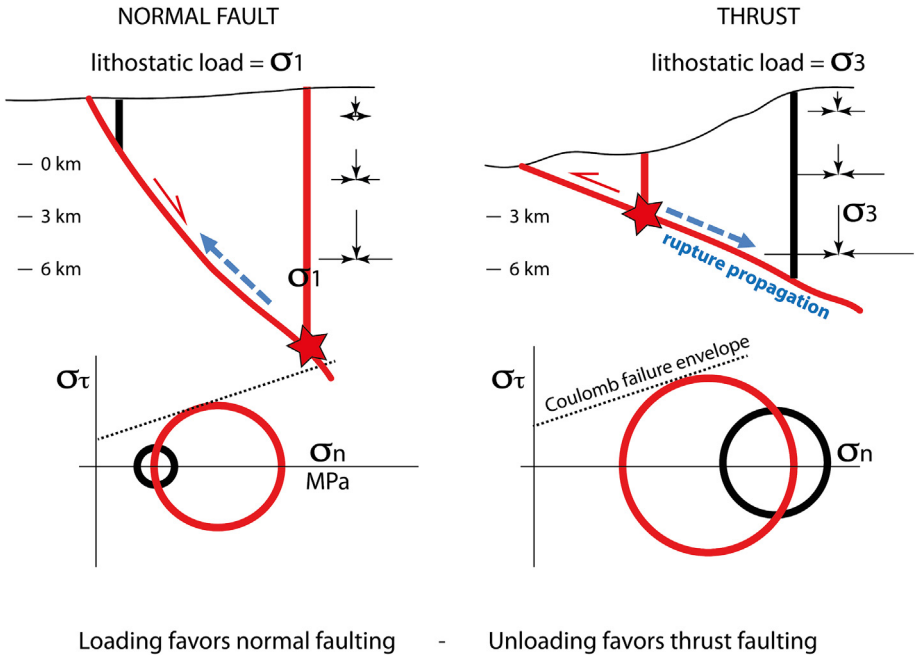

Fig. 8. The lithostatic load is the maximum principal stress in extensional tectonic settings, whereas it is the minimum principal stress in contractional tectonic settings. This facilitates rupture at depth and upward migration of aftershocks along normal faults, whereas it triggers shallow rupture and downward migration of coseismic slip and aftershocks along thrust planes.

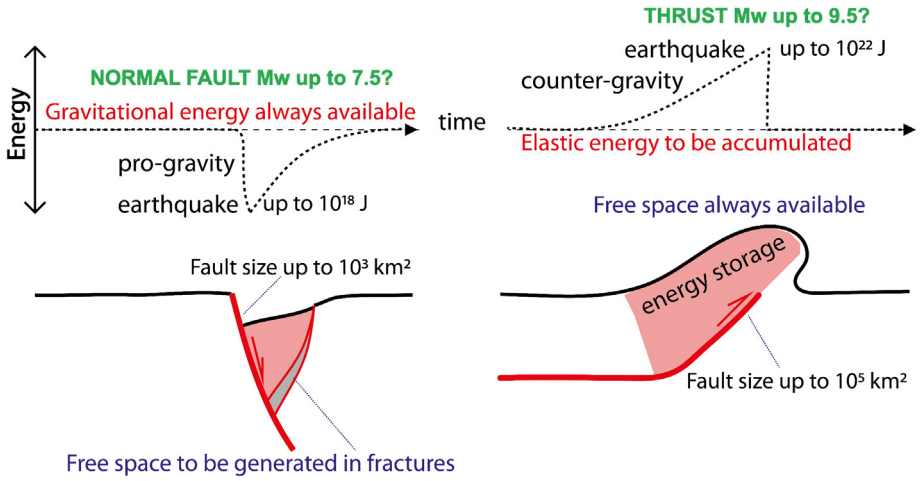

Fig. 9. The energy determining earthquakes is mostly stored in the hanging walls of thrusts and normal faults and in the volumes adjacent to strike-slip faults. However, the dissipation of gravitational energy characterizes normal faults, whereas elastic energy is required to move the volume upward. In extensional settings the gravitational energy is always active, whereas the crustal dilation space where the volume can move downward at the coseismic stage must be generated during the interseismic period. The opposite occurs in contractional settings where the elastic energy must be accumulated during the interseismic period and the free surface where to move the volume at the coseismic stage is permanently available.

et al., 2011). For a review of this opposite pattern see Carminati et al. (2004). All this supports the evidence that the energy determining fault motion in both tectonic settings is stored in the hanging wall volume but with different contributions, i.e., gravitational for normal faulting and elastic in contractional settings.

5. Conclusions

Starting from a steady state evolution, the preparation of fault activation needs delivering gravitational energy for extensional tectonic settings, whereas it requires elastic energy to accumulate the force for moving the volume against gravity (Fig. 8).

Therefore, different energy accumulation occurs in the three main tectonic settings during the interseismic preparatory phase of earthquakes (Fig. 9). In extensional regimes, the gravitational energy is already in the volume (pro-gravity), but the potential energy increases as the dilatational antithetic wedge grows in the hangingwall of the normal fault as predicted in Doglioni et al. (2011) and proved by InSAR analysis by Valerio et al. (2018) and Bignami et al. (2019). Strike-slip settings generate faults and motions mostly horizontally (iso-gravity) and the dimension of the volume storing energy depends on the strain rate between the two walls (Zaccagnino and Doglioni, 2022b). In contractional tectonic settings, the elastic energy is gradually stored during the interseismic preparatory phase (counter-gravity) until the critical stage is reached and the static friction along the fault plane is overtaken (Fig. 10). Since the movement occurs against gravity, once the main energy budget is dissipated, the hangingwall cannot move upward anymore and this explains the shorter duration of compressive seismic sequences with respect to the extensional ones (Valerio et al., 2017).

Therefore, the differential stress required to activate a normal fault system is lower than strike-slip and contractional faults because the hanging wall volume moves in favor of gravity. The lower differential stress required for activating normal faults is usually interpreted because rupturing rocks under contraction requires far more energy than under traction. This assumption is correct at the Earth's surface, but not in the crust beneath 1 km (e.g., Brudy et al., 1997); below that depth, rocks are under compression also in extensional tectonic settings due to the confining pressure of the lithostatic load. Here is shown that the differential stress is larger in contractional tectonic settings because the hang-

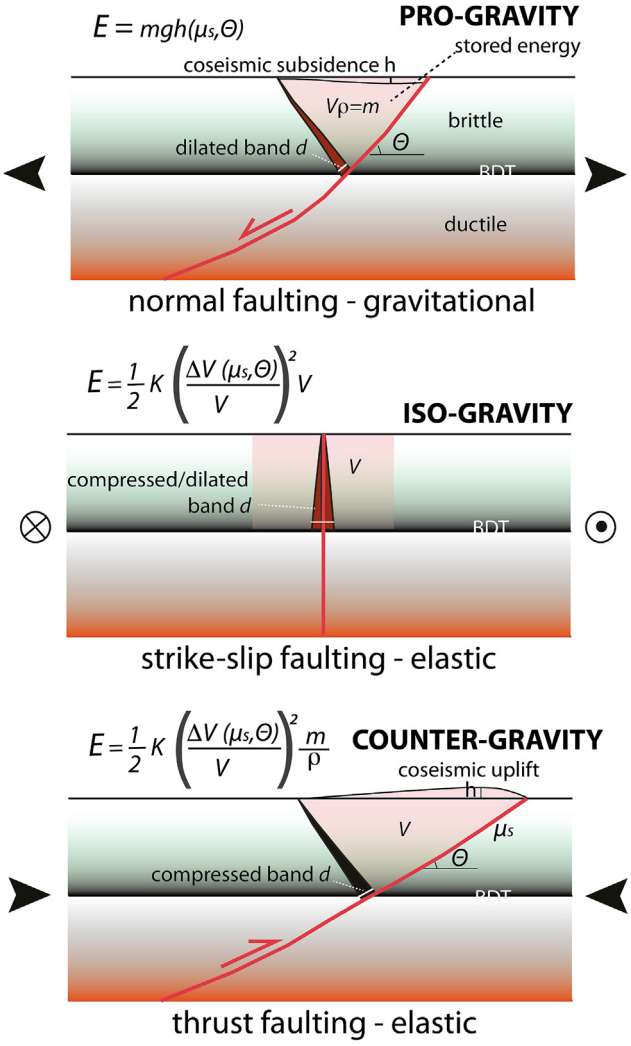

E = energy, *m* = mass, ρ = density, *K* = bulk modulus, μ_s = static friction
V = volume, *d* = displacement, Θ = fault dip, *h*=*d*sin(Θ), *g* = gravity

Fig. 10. Different tectonic settings and related interseismic energy accumulation are dictated by the relation with gravity (modified after Doglioni et al., 2015b).

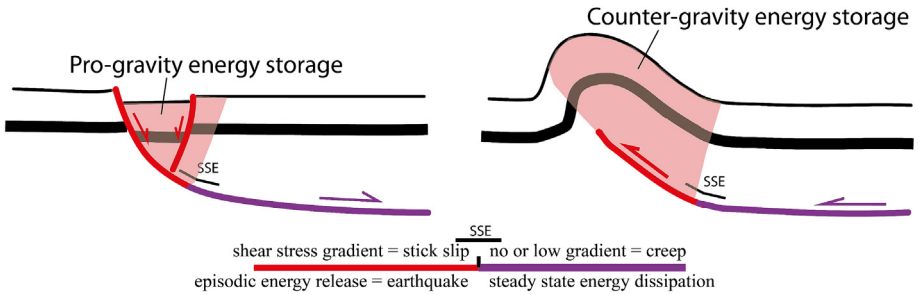

Fig. 11. The shaded red areas represent the volumes above locked faults where the energy accumulates during the interseismic cycle due to the moving volume above the creeping shear zones. The energy is gravitational in the extensional setting to the left, whereas it is elastic in the contraction setting to the right. SSE, the possible location of slow-slip events (modified after Zaccagnino and Doglioni, 2023).

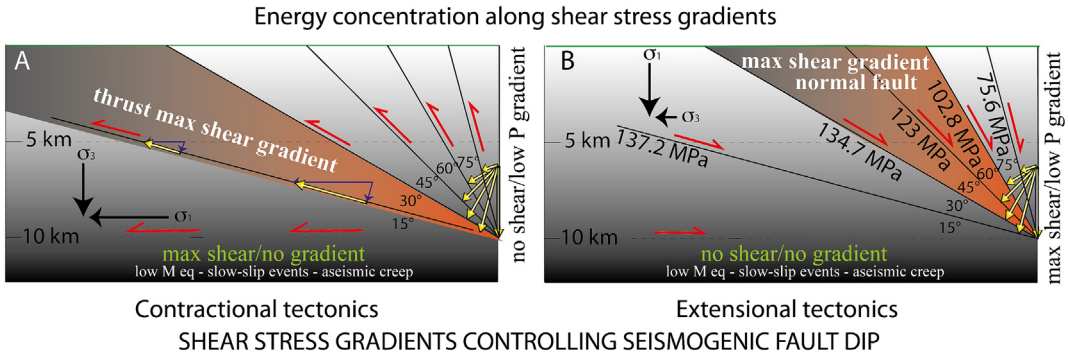

Fig. 12. The dip of faults allowing the hanging wall volume to move during the coseismic stage is controlled by the zones where it forms the higher shear stress gradient in the interseismic period. Numbers in panel (b) indicate the normal stress variation at 5 km depth acting on the fault plane as a function of the normal fault dip due to the lithostatic load (modified after Zaccagnino and Doglioni, 2023).

ing wall volume moves against gravity, i.e., requiring much larger energy with respect to extensional tectonics. All related seismological parameters follow this energetic constraint, for example the interseismic larger number of earthquakes of low magnitude in extensional tectonic settings and having larger and lastly longer aftershocks following a normal fault-related mainshock with respect to contractional areas with similar strain rate. Extensional settings have shorter spacing among normal faults, thicker fault damage zones, lower fractal numbers (Fig. 5), and lower double couple (Zaccagnino and Doglioni, 2022a). In all tectonic settings, the energy is stored in the volume adjacent to faults. The seismogenic fault or faults system represents the weak zones of the volume where the seismic radiation occurs starting from the weakest area of the main fault plane (e.g., Bird and Kong, 1994). For the above reasons, the earthquakes should be differentiated also on the basis of their source of energy stored in the volumes, which is in fact controlling both their specific evolution and nucleation, i.e., graviquakes for earthquakes occurring in extensional tectonic settings (pro-gravity), and elastoquakes for the earthquakes generating in strike-slip and contractional settings (iso- and counter-gravity). Moreover, the energy is mostly stored in the volumes surrounding the main fault, specifically the hanging wall in extensional and contractional settings (Fig. 11) and faults activate along the dip where it is concentrated the highest shear stress gradient (Fig. 12). In the seismic cycle, during the interseismic period occur mostly the upper left, lower energy events of the Gutenberg-Richter frequency/magnitude relationship, whereas the mainshock and the related aftershocks fill the *b*-value in the lower right of the alignment (Fig. 13).

Therefore, since energy activating crustal volumes and related faults, is different as a function of the tectonics setting, i.e., gravitational in extensional tectonic settings moving in favour of gravity, and elastic in all other tectonic settings, the maximum magnitude is smaller for normal fault requiring less external energy. In extensional settings, the volume dimension is given by the thickness of the brittle layer, and its length is about three times

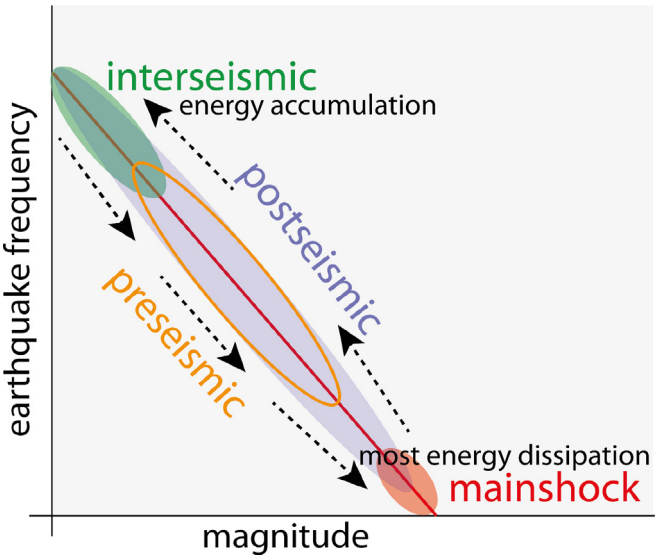

Fig. 13. Temporal evolution of earthquake distribution moves along the Gutenberg-Richter *b*-value trend, being the low magnitude events more abundant in the interseismic preparatory phase and during the aftershocks energy dissipation. The lower right of the alignment concentrates mostly during the coseismic stage when most of the energy is delivered by the mainshock and related decay via elevated magnitude aftershocks.

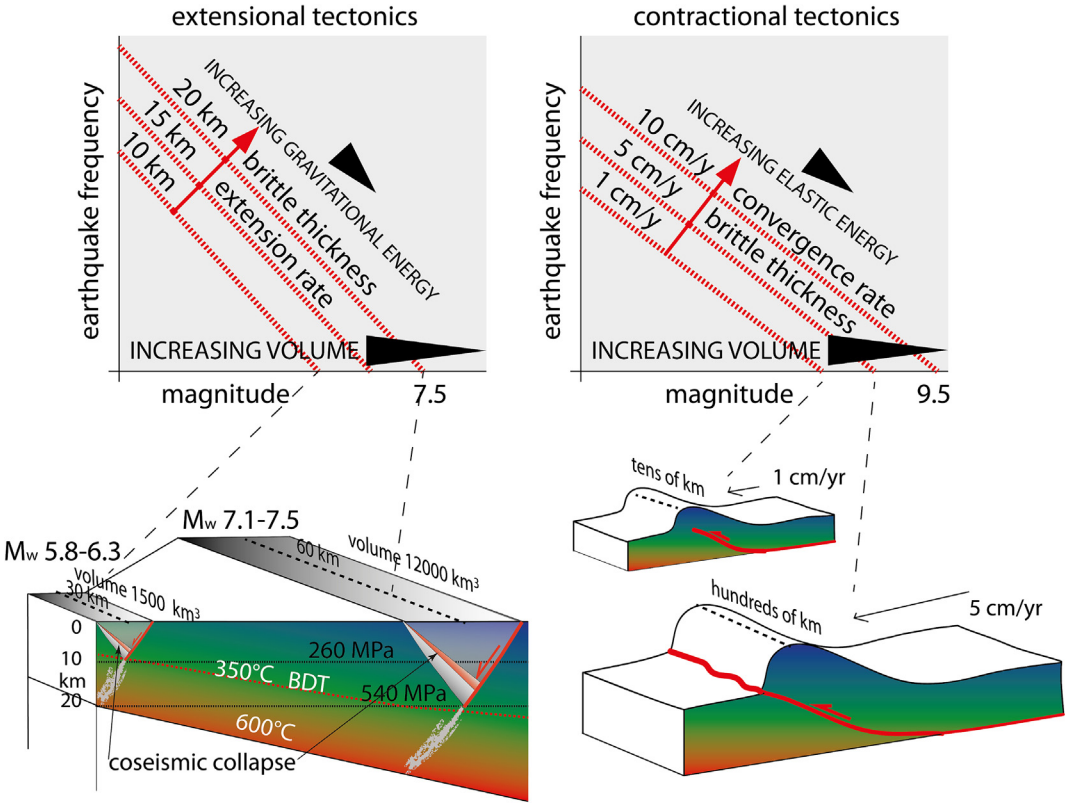

Fig. 14. In the upper panels, the red dashed lines represent the *b*-value of the Gutenberg–Richter law, which is steeper in extensional tectonic settings and is shifted upward (i.e., stronger magnitudes) depending on the seismogenic brittle thickness; gravitational energy dominates. The temporal recurrence of normal fault earthquakes depends on the extensional rate. In contractional tectonic settings, the *b*-value is rather less inclined, and magnitudes can be much higher due to the larger energy required to move upward bigger crustal volumes. The frequency/magnitude relation moves upward, and the magnitude increases as a function of the contractional rate and the involved volume; elastic energy dominates. In extensional settings there are more low-magnitude earthquakes. In these settings the volume moves down in favor of gravity; vice versa, in contractional tectonic settings, the volume moves against gravity and the number of low-magnitude earthquakes is smaller, accumulating more elastic energy to move up the hanging-wall volume. In all tectonic settings, the magnitude scales with the volumes involved. The lower panels exemplify the volume and magnitude differences in extensional and contractional tectonic settings. Notice that $M \geq 9$ in contractional settings occur only along widespread subduction zones at plates interface with the convergence rate of at least a few cm/yr.

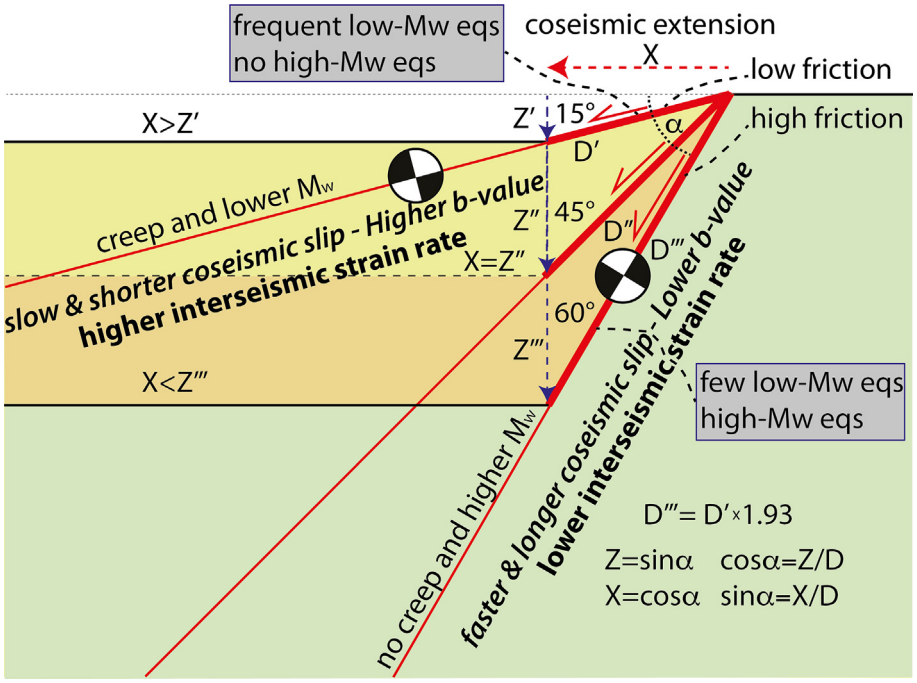

Fig. 15. At a given coseismic extension, the dip of extensional fault determines the amount of vertical displacement, being the dip controlled by the internal friction of rocks. Therefore, the steeper the fault, the longer the coseismic displacement, the faster the hangingwall collapses and the larger the magnitude generated by the gravitational energy (graviquake). Low friction rocks determine interseismic higher strain rate and vice versa.

the seismogenic thickness, whereas in the strike-slip and contractional settings, where the elastic energy dominates (elastoquakes) the volume may be ten to thirty times longer, being its size proportional both to the brittle thickness and the relative speed of plates (Doglioni et al., 2015a). The magnitude increases with the volume and, therefore, with the thickness of the seismogenic layer. The strain rate controls the recurrence of the events (Fig. 14). In contractional tectonic settings, the magnitude rather increases with the speed of the convergence rate, which determines the volume dimension and the higher energy required to move the crustal volume against gravity (Fig. 14). The energy generating tectonics and related seismicity is given by the interplay between the horizontal plate tectonics forces and the lithostatic load, which is ubiquitous. The horizontal shear stress is rather concentrated within given crustal/lithospheric volumes where horizontal plate velocity gradients concentrate. The energy varies in the three main tectonic settings, generating different seismotectonic styles. With a given strain rate and crustal thickness, the seismic energy increases as the effect of the vertical gravitational force becomes a minority, especially when the crust is pushed upward against gravity. Horizontal tectonic forces interact with the lithostatic load, which is omnipresent. The energy budget and the resulting magnitude vary in the three main tectonic settings, and the classification of graviquakes and elastoquakes is finalized to distinguish their different role. Strike-slip and contractional settings may store energy in bigger volumes, hence providing the activation of wider faults and larger earthquakes. The quicker the fault motion, the stronger the release of the elastic waves. Normal faults show higher seismic energy dissipation as the fault becomes steeper: at a given extensional strain rate, the steeper the fault, the larger the gravitational displacement; the longer the fault displacement and the faster the coseismic slip (Fig. 15). In fact, no major earthquakes may occur along low angle normal faults (Jackson and White, 1989; Doglioni et al., 2015a, 2015b).

CRediT authorship contribution statement

Carlo Doglioni: Conceptualization, Writing original draft, Resources, Methodology, Investigation, Formal analysis, Data curation, Review & editing.

Declaration of Competing Interest

The author declares that he has no known competing financial interests or personal relationships that could have appeared to influence the work reported in this paper.

Acknowledgments

I thank Davide Zaccagnino for useful and stimulating discussions. Two anonymous referees and the Associate Editor provided very helpful comments. The research was supported by Istituto Nazionale di Geofisica e Vulcanologia (INGV) and Sapienza University of Rome.

References

Allerton, S., Murton, B.J., Searle, R.C., Jones, M., 1995. Extensional faulting and segmentation of the Mid-Atlantic Ridge north of the Kane Fracture Zone (24°00′N to 24°40′N). Marine Geophys. Res. 17, 37–61.
Bath, M., 2013. Introduction to Seismology (Vol. 27). Birkhäuser.
Beanland, S., Blick, G.H., Darby, D.J., 1990. Normal faulting in a back arc basin: geological and geodetic characteristics of the 1987 Edgecumbe earthquake, New Zealand. J. Geophys. Res. Solid Earth 95 (B4), 4693–4707.
Ben-Zion, Y., Sammis, C.G., 2003. Characterization of fault zones. Pure Appl. Geophys. 160 (3), 677–715.
Bignami, C., Valerio, E., Carminati, E., Doglioni, C., Tizzani, P., 2019. Volume unbalance on the 2016 Amatrice-Norcia (central Italy) seismic sequence and insights on normal fault earthquake mechanism. Sci. Rep. 9, 4250. https://doi.org/10.1038/s41598-019-40958-z.
Bignami, C., Valerio, E., Carminati, E., Doglioni, C., Petricca, P., Tizzani, P., Lanari, R., 2020. Are normal fault earthquakes due to elastic rebound or gravitational collapse? Ann. Geophys. 63 (2), SE213. https://doi.org/10.4401/ag-8455.
Bird, P., Kong, X., 1994. Computer simulations of California tectonics confirm very low strength of major faults. Geol. Soc. Am. Bull. 106 (2), 159–174.
Biswas, S., Ray, P., Chakrabarti, B.K., 2015. Statistical Physics of Fracture, Breakdown, and Earthquake: Effects of Disorder and Heterogeneity. John Wiley & Sons.
Boyer, S.E., 1995. Sedimentary basin taper as a factor controlling the geometry and advance of thrust belts. Am. J. Sci. 295 (10), 1220–1254.
Boyer, S.E., Elliott, D., 1982. Thrust systems. Am. Ass. Petrol. Geol. Bull. 66 (9), 1196–1230.
Brudy, M., Zoback, M., Fuchs, K., Rummel, F., Baumgärtner, J., 1997. Estimation of the complete stress tensor to 8 km depth in the KTB scientific drill holes: Implications for crustal strength. J. Geophys. Res. Solid Earth 102 (B8), 18453–18475.
Carminati, E., Doglioni, C., Barba, S., 2004. Reverse migration of seismicity on thrusts and normal faults. Earth-Sci. Rev. 65 (3–4), 195–222.
Chen, W., Rao, G., Kang, D., Wan, Z., Wang, D., 2023. Early report of the source characteristics, ground motions, and casualty estimates of the 2023 Mw 7.8 and 7.5 Turkey earthquakes. J. Earth Sci. 34 (2), 297–303.
Chiarabba, C., De Gori, P., Valoroso, L., Petitta, M., Carminati, E., 2022. Large extensional earthquakes push-up terrific amount of fluids. Sci. Rep. 12 (1), 14597. https://doi.org/10.1038/s41598-022-18688-6.
Cocco, M., Rovelli, A., 1989. Evidence for the variation of stress drop between normal and thrust faulting earthquakes in Italy. J. Geophys. Res. Solid Earth 94 (B7), 9399–9416.
Doglioni, C., Barba, S., Carminati, E., Riguzzi, F., 2011. Role of the brittle-ductile transition on fault activation. Phys. Earth Planet. Int. 184, 160–171.
Doglioni, C., Panza, G., 2015. Polarized Plate Tectonics. Advances in Geophysics, vol. 56. Elsevier, pp. 1–167.
Doglioni, C., Barba, S., Carminati, E., Riguzzi, F., 2014. Fault on–off versus coseismic fluids reaction. Geosci. Front. 5 (6), 767–780.
Doglioni, C., Carminati, E., Petricca, P., Riguzzi, F., 2015a. Normal fault earthquakes or graviquakes. Sci. Rep. 5 (1), 12110. https://doi.org/10.1038/srep12110.
Doglioni, C., Barba, S., Carminati, E., Riguzzi, F., 2015b. Fault on-off versus strain rate and earthquakes energy. Geosci. Front. 6, 265–276. https://doi.org/10.1016/j.gsf.2013.12.007.
Hatano, T., Narteau, C., Shebalin, P., 2015. Common dependence on stress for the statistics of granular avalanches and earthquakes. Sci. Rep. 5, 12280.
Holschneider, M., Narteau, C., Shebalin, P., Peng, Z., Schorlemmer, D., 2012. Bayesian analysis of the modified Omori law. J. Geophys. Res. 117, B06317.
Jackson, J.A., White, N.J., 1989. Normal faulting in the upper continental crust: observations from regions of active extension. J. Struct. Geol. 11 (1–2), 15–36. https://doi.org/10.1016/0191-8141(89)90033-3.
Jiménez, C., 2018. Seismic source characteristics of the intraslab 2017 Chiapas-Mexico earthquake (Mw8. 2). Phys. Earth Planet. Int. 280, 69–75.
Johnson, S.E., Song, W.J., Vel, S.S., Song, B.R., Gerbi, C.C., 2021. Energy partitioning, dynamic fragmentation, and off-fault damage in the earthquake source volume. J. Geophys. Res. Solid Earth 126 (11). 2021JB022616.
Kagan, Y., 1991. Fractal dimension of brittle fracture. J. Nonlinear Sci. 1 (1), 1–16. https://doi.org/10.1007/BF01209146.
Kanamori, H., 1994. Mechanics of earthquakes. Ann. Rev. Earth Planet. Sci. 22, 207–237.
Kanamori, H., Rivera, L., 2006. Energy partitioning during an earthquake. In: Abercrombie, R., et al. (Eds.), Earthquakes: Radiated Energy and the Physics of Faulting. Am. Geophys. Un., Geophys. Monograph Series 170, 3-13.
Kanamori, H., Brodsky, E.E., 2004. The physics of earthquakes. Rep. Prog. Phys. 67 (8), 1429.
Koketsu, K., Yokota, Y., Nishimura, N., Yagi, Y., Miyazaki, S.I., Satake, K., Fujii, Y., Miyake, H., Sakai, S.I., Yamanaka, Y., Okada, T., 2011. A unified source model for the 2011 Tohoku earthquake. Earth Planet. Sci. Lett. 310 (3–4), 480–487.
Lay, T., 2018. A review of the rupture characteristics of the 2011 Tohoku-oki Mw 9.1 earthquake. Tectonophysics 733, 4–36.
Lay, T., Kanamori, H., Ammon, C.J., Nettles, M., Ward, S.N., Aster, R.C., Beck, S.L., Bilek, S.L., Brudzinski, M.R., Butler, R., DeShon, H.R., 2005. The great Sumatra-Andaman earthquake of 26 December 2004. Science 308 (5725), 1127–1133.
Li, J., Kim, T., Lapusta, N., Biondi, E., Zhan, Z., 2023. The break of earthquake asperities imaged by distributed acoustic sensing. Nature 620 (7975), 800–806.
McBeck, J., Ben-Zion, Y., Renard, F., 2022. Volumetric and shear strain localization throughout triaxial compression experiments on rocks. Tectonophysics 822, 229181.
Morellato, C., Redini, F., Doglioni, C., 2003. On the number and spacing of faults. Terra Nova 15 (5), 315–321.
Morley, C.K., 1988. Variable extension in Lake Tanganyika. Tectonics 7 (4), 785–801. https://doi.org/10.1029/TC007i004p00785.
Muir Wood, R., 1994. Earthquakes, strain-cycling and the mobilization of fluids. Geol. Soc., London, Special Publications 78 (1), 85–98.
Muir-Wood, R., King, G.C.P., 1993. Hydrological signatures of earthquake strain. J. Geophys. Res. 98 (B12), 22035–22068.
Narteau, C., Shebalin, P., Holschneider, M., 2002. Temporal limits of the power law aftershock decay rate. J. Geophys. Res. 107, B122359.

Narteau, C., Byrdina, S., Shebalin, P., Schorlemmer, D., 2009. Common dependence on stress for the two fundamental laws of statistical seismology. Nature 462, 642–645.
Okubo, K., Bhat, H.S., Rougier, E., Marty, S., Schubnel, A., Lei, Z., Knight, E.E., Klinger, Y., 2019. Dynamics, radiation, and overall energy budget of earthquake rupture with coseismic off-fault damage. J. Geophys. Res., Solid Earth 124 (11), 11771–11801.
Pearson, C., Beavan, J., Darby, D., Blick, G., Walcott, R., 1995. Strain distribution across the Australian-Pacific plate boundary in the central South Island, New Zealand, from 1992 GPS and earlier terrestrial observations. J. Geophys. Res. Solid Earth 100 (B11), 22071–22081.
Petricca, P., Bignami, C., Doglioni, C., 2021. The epicentral fingerprint of earthquakes marks the coseismically activated crustal volume. Earth-Sci. Rev. 218, 103667.
Petricca, P., Carminati, E., Doglioni, C., 2022. Estimation of the maximum earthquakes magnitude based on potential brittle volume and strain rate: the Italy test case. Tectonophysics. https://doi.org/10.1016/j.tecto.2022.229405.
Petruccelli, A., Schorlemmer, D., Tormann, T., Rinaldi, A.P., Wiemer, S., Gasperini, P., Vannucci, G., 2019. The influence of faulting style on the size-distribution of global earthquakes. Earth Planet. Sci. Lett. 527, 115791.
Pollitz, F., Banerjee, P., Grijalva, K., Nagarajan, B., Bürgmann, R., 2008. Effect of 3-D viscoelastic structure on post-seismic relaxation from the 2004 M= 9.2 Sumatra earthquake. Geophys. J. Int. 173 (1), 189–204.
Reid, H.F., 1911. The elastic-rebound theory of earthquakes. Univ. Calif. Publ. Bull. Dept. Geol. 6 (19), 413–444.
Riguzzi, F., Crespi, M., Devoti, R., Doglioni, C., Pietrantonio, G., Pisani, A.R., 2012. Geodetic strain rate and earthquake size: New clues for seismic hazard studies. Phys. Earth Planet. Int. 206–207, 67–75.
Scholz, C.H., 2019. The Mechanics of Earthquakes and Faulting. Cambridge University Press.
Schorlemmer, D., Wiemer, S., Wyss, M., 2005. Variations in earthquake-size distribution across different stress regimes. Nature 437 (7058), 539–542.
Searle, R.C., Murton, B.J., Achenbach, K., LeBas, T., Tivey, M., Yeo, I., Cormier, M.H., Carlut, J., Ferreira, P., Mallows, C., Morris, K., 2010. Structure and development of an axial volcanic ridge: Mid-Atlantic Ridge, 45°N. Earth Planet. Sci. Lett. 299 (1–2), 228–241.
Shebalin, P., Narteau, C., 2017. Depth dependent stress revealed by aftershocks. Nature Comm. 8, 1317.
Sibson, R.H., 1974. Frictional constraints on thrust, wrench and normal faults. Nature 249 (5457), 542–544.
Sibson, R., 1977. Fault rocks and fault mechanisms. J. Geol. Soc. 133 (3), 191–213.
Sornette, D., 1999. Earthquakes: from chemical alteration to mechanical rupture. Phys. Rep. 313 (5), 237–292.
Stein, S., Wysession, M., 2009. An Introduction to Seismology, Earthquakes, and Earth Structure. John Wiley & Sons.
Taroni, M., Carafa, M.M.C., 2023. Earthquake size distributions are slightly different in compression vs extension. Comm. Earth Environ. 4, 398. https://doi.org/10.1038/s43247-023-01059-y.
Telesca, L., Lapenna, V., 2006. Measuring multifractality in seismic sequences. Tectonophysics 423 (1–4), 115–123.
Thompson, G.A., Parsons, T., 2017. From coseismic offsets to fault-block mountains. Proc. Nat. Acad. Sci. 114 (37), 9820–9825.
Twiss, R.J., Moores, E.M., 1992. Structural Geology. Macmillan.
Valerio, E., Tizzani, P., Carminati, E., Doglioni, C., 2017. Longer aftershocks duration in extensional tectonic settings. Sci. Rep. 7 (1), 16403. https://doi.org/10.1038/s41598-017-14550-2.
Valerio, E., Tizzani, P., Carminati, E., Doglioni, C., Pepe, S., Petricca, P., De Luca, C., Bignami, C., Solaro, G., Castaldo, R., De Novellis, V., 2018. Ground deformation and source geometry of the 30 October 2016 M_w 6.5 Norcia earthquake (central Italy) investigated through seismological data, DInSAR measurements, and numerical modelling. Remote Sens. 10 (12), 1901.
Zaccagnino, D., Doglioni, C., 2022a. The impact of faulting complexity and type on earthquake rupture dynamics. Comm. Earth. Env. 3 (1), 258. https://doi.org/10.1038/s43247-022-00593-5.
Zaccagnino, D., Doglioni, C., 2022b. Earth's gradients as the engine of plate tectonics and earthquakes. La Rivista Del Nuovo Cimento 45 (12), 801–881.
Zaccagnino, D., Doglioni, C., 2023. Fault dip vs shear stress gradient. Geosystems and Geoenvironment 2 (4), 100211. https://doi.org/10.1016/j.geogeo.2023.100211.
Zaccagnino, D., Telesca, L., Doglioni, C., 2022. Scaling properties of seismicity and faulting. Earth Planet. Sci. Lett. 584, 117511.
Zoback, M.D., Apel, R., Baumgärtner, J., Brudy, M., Emmermann, R., Engeser, B., Fuchs, K., Kessels, W., Rischmüller, H., Rummel, F., Vernik, L., 1993. Upper-crustal strength inferred from stress measurements to 6 km depth in the KTB borehole. Nature 365 (6447), 633–635.